

**O8-4****DEPTH DISTRIBUTION OF STRESSES IN THE HOKKAIDO WADATI-BENIOFF ZONE AS DEDUCED BY INVERSION OF EARTHQUAKE FOCAL MECHANISMS****CENKA CHRISTOVA<sup>1</sup> and THEODOROS TSAPANOS<sup>2</sup>**<sup>1</sup> Geophysical Institute of Bulgarian Academy of Sciences, Dept. of Seismology, Acad.G. Bonchev str. Bl.3 Sofia 1113, Bulgaria.<sup>2</sup> Aristotle University of Thessaloniki, Geophysical Lab., 54006 Thessaloniki, Greece.

The paper focuses on the depth distribution of stresses in the Hokkaido Wadati-Benioff zone. The considered area is limited by the parallels 40°-48°N and meridians 140°-150°E. It comprises the southernmost part of the Kurile Island and Hokkaido where the active subduction of the Pacific plate beneath the Eurasian continent results in an well-defined Wadati-Benioff zone.

The morphology of the Hokkaido Wadati-Benioff zone (**HWBZ**) was studied in details by Hanus and Vanek (1984). According to their study the **HWBZ** dips to NW at 40°, its prevailing thickness is of about 50 km, maximum depth of penetration is of 270 km. An intermediate depth seismic gap in the **HWBZ** in the depth range 90-215 km and its close relation to active andesitic volcanism was confirmed. The geometry of an activated paleosubduction zone (**HPSZ**) of variable dip and thickness in the depth range 220-560 km was also outlined.

Based on knowledge of the geometry of the deep seismogenic structures in the studied region, we were able to distinct 217 earthquakes (with available CMT Harvard solutions) which belong to the **HWBZ** and 13 for the **HPSZ**. An epicentral map of the earthquakes used in our study is shown in Figure 1. In the further procedure, we used the inverse technique of Gephart and Forsyth (1984) for determining the best fit principle stress directions  $\sigma_1$ ,  $\sigma_2$ ,  $\sigma_3$  and the ratio  $R = \sigma_2 - \sigma_1 / \sigma_3 - \sigma_1$  for 20 km depth intervals in the **HWBZ** and for the **HPSZ** considered as a whole body. The results obtained as well as the misfit of the best stress models are listed in Table 1.

In almost all considered depth layers the maximum compressive stresses  $\sigma_1$  are normal to the strike of the slab and dip less than 25°, indicating the NW-SE convergence between the Pacific and Eurasian lithospheric plates. Exclusions are: the depth layer 81-120 km with almost along strike  $\sigma_1$ ; 161-220 km where  $\sigma_1$  towards E and is almost horizontal; and **HPSZ**. With down dipping  $\sigma_1$ . The minimum compressive stresses  $\sigma_3$  are down dipping only at depth 21-60 km. In all reminder depth intervals  $\sigma_3$  are along the strike of the slab and of different dips.

These results indicate that the slab pull and the mantle resistance acting on the slab edge are not the only forces which control the contemporary plate tectonics in the Hokkaido region. Along strike compression at depths 81-120 km and along strike extension at 0-20 and 61-220 km are involved in the slab dynamics. These can be related to horizontal bending of the subducting Pacific plate.

**Referances**

- Gephart, J. and Forsyth, D., 1984. An improved method for determining the regional stress tensor using earthquake focal mechanism data: application to the San Fernando earthquake sequence. *J. Geophys. Res.*, 89: 9305-9320.
- Hanus, V. and Vanek, J., 1984. Earthquake distribution and volcanism in Kamchatka, Kurile islands, and Hokkaido. Part 3: Southern Kuriles and Hokkaido, *Studia geoph. Et geod.*, 28: 248-271.

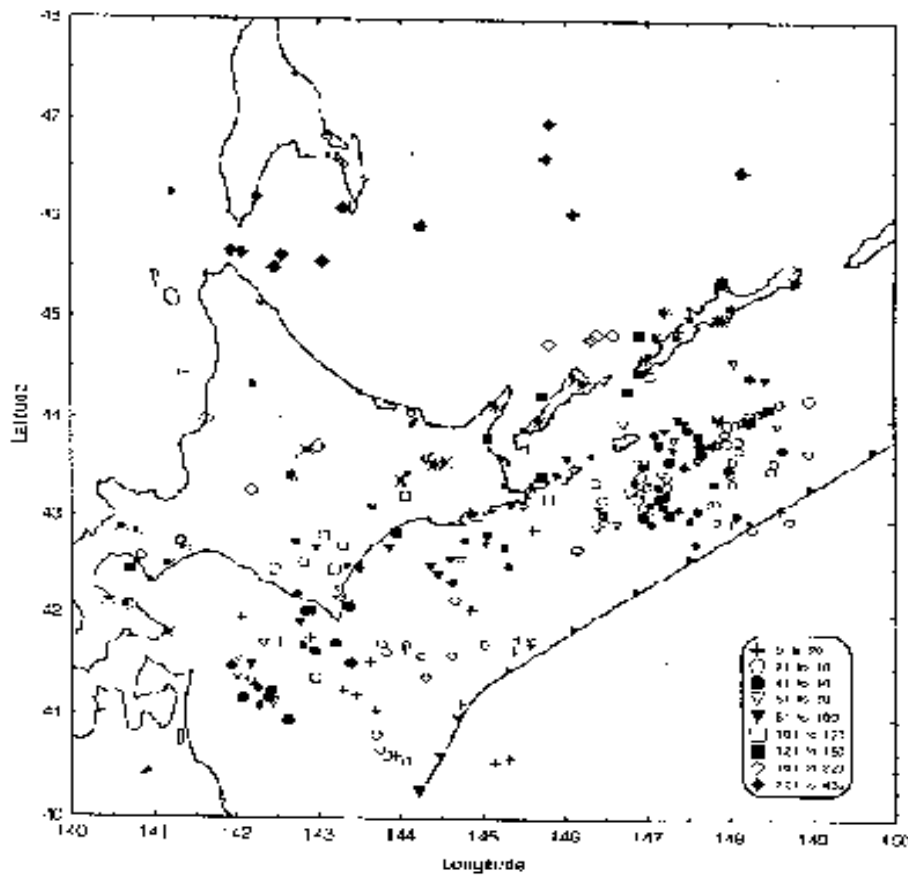


Figure 1. Epicentral map of earthquakes which focal mechanisms were used for determining the stress field parameters in the Hokkaido Wadati-Benioff zone. The symbols used for the considered depth ranges are listed in the legend. The trench is marked by a serrate line, the active volcanic volumes by stars.

Table 1. Best fit stress models for the Hokkaido Wadati-Benioff zone. N is the number of earthquake focal mechanisms used; the following three columns show the directions (dip/azimuth) of the principle stresses  $\sigma_1$ ,  $\sigma_2$ ,  $\sigma_3$ ; the next columns include the value of R and the average misfit  $\theta$  for the best model.

Depth [km]	N	$\sigma_1$ dip/azimuth	$\sigma_2$ dip/azimuth	$\sigma_3$ dip/azimuth	R	$\theta$ misfit
0 - 20	25	17/112	58/130	27/13	0.70	9.89
21 - 40	57	22/125	57/32	67/282	0.60	4.05
41 - 60	60	0/155	62/16	50/45	0.50	5.25
61 - 80	25	17/126	20/224	61/3	0.70	5.38
81 - 100	22	67/169	5/281	21/15	0.70	8.34
101 - 120	10	39/70	6/105	50/7	0.30	4.22
121 - 160	8	20/130	68/281	9/37	0.90	4.33
161 - 220	10	3/64	62/183	27/357	0.40	4.16
subarc reaction	13	-3/261	2/142	30/30	0.40	5.35

